Electron emission and electronic stopping in the interaction of slow helium ions with aluminum

P. Riccardi*
Dipartimento di Fisica, Università della Calabria and INFN–Gruppo Collegato di Cosenza, Via P. Bucci Cubo 33C, Arcavacata di Rende, Cosenza, Italy

R. A. Baragiola† and C. A. Dukes
Engineering Physics, University of Virginia, Charlottesville, Virginia 22904, USA
(Received 20 July 2014; revised manuscript received 2 June 2015; published 23 July 2015)

We address the question of the nonlinearity of the electronic stopping power of slow helium ions in aluminum by measuring the energy distributions and yields of electron emission under the impact of 0.2–4.5 keV $^3He^+$ and $^4He^+$ ions. Electron emission experiments can provide an alternative point of view to resolve controversial issues often arising in stopping power measurements. The comparison between two isotopes allows one to distinguish between the energy and velocity dependent emission mechanisms, and indicates that the reported nonlinear velocity dependence of the electronic stopping power can be attributed to residual nuclear stopping effects.

DOI: 10.1103/PhysRevB.92.045425 PACS number(s): 79.20.Rf, 34.50.Bw, 61.80.Jh

I. INTRODUCTION

Electronic processes that occur when atomic particles move through solid materials are of importance in many areas of research and technology, including astrophysics, plasma physics, materials science, and biomedical research [1,2]. The key quantity to investigate these processes is the electronic stopping power S_e, i.e., the energy loss to the electrons per unit length traveled by the projectile. For a free electron gas, the electronic stopping power of a light ion moving with velocity lower than the Fermi velocity is expected to be proportional to the particle velocity, $S_e = Q(Z_1, r_s)v$, where the "friction coefficient" Q is peculiar to the projectile-target system, and depends on the atomic number of the ion Z_1 and on the electron density of the free electron gas n_e, expressed in terms of the Wigner-Seitz radius, $r_s = (3/4\pi n_e)^{1/3}$. Such behavior has been reported experimentally for light ions in metals and in particular in the electronic stopping power of He in Al measured in the transmission method [3]. In contrast, a surprising deviation from linearity and a much smaller S_e at low velocity has been reported recently in measurements of the electronic stopping power of He ions backscattered from nanometer thick polycrystalline Al films grown on Ta substrates [4]. The reason for this nonlinearity was proposed to be the charge exchange processes due to the repeated promotion of the $1s$ level of He when close to the Al cores [4].

Ions also transfer kinetic energy to the nuclei, and the total stopping power S, which is the quantity measured in experiments, is defined as the sum $S = S_e + S_n$, where S_n is the nuclear stopping power. At low projectile velocity both the nuclear and electronic stopping are sizable and the disentanglement of S_n from the measured S to obtain S_e is not a trivial task [5]. It has been suggested that the discrepancy at low velocity between the different measurements of S_e for the He-Al system could be due to an underestimation of S_n in the measurements performed in the transmission geometry [6]. However, calculations of the electronic stopping power by time dependent density functional theory (TDDFT) [7–9], which do not include promotion effects, appear to be consistent with the measurements in the transmission geometry [3,9].

Electron emission is another outcome of the inelastic processes that can be studied in detail. Ion-induced electron emission processes are grouped into the two main categories of potential electron emission (PEE) and kinetic electron emission (KEE), due respectively to the transfer to the solid of the potential and the kinetic energy brought by the incoming particle [10,11]. As outlined in Ref. [12], in many cases electronic energy loss and electron emission are strictly related and KEE yields γ (the number of emitted electrons per incident ion) are found to be proportional to the electronic stopping power for slow light ions [12]. Moreover, impact parameter dependent effects, such as electron promotion in close atomic encounters, occur at impact energies above a threshold that is peculiar to the collision system and often promote electrons above the vacuum level, resulting in electron emission that produces features in the energy distributions and in the yield curve of emitted electrons [13,14].

As mentioned above, the experimental curves of the electronic stopping power for the He-Al system [3,4] are in good agreement at high impact energies, above about 10 keV. In this range of impact energies both the measured electronic stopping powers are proportional to the experimental KEE yields [12]. Therefore, to answer the question of the linearity of the electronic stopping of helium ions in aluminum, we studied electron emission, aiming at the clarification of the emission mechanisms. We measured energy distributions and yields of electrons emitted in the interaction of ^3He ions with a polycrystalline Al surface. A comparison with the most commonly used $^4He^+$ ions shows that mechanisms of electron excitation and emission are the same for the two isotopes, crucially allowing one to distinguish between the energy and velocity dependent effects. The experiments show that electron promotion effects do not produce a significant contribution and the KEE yields for the impact of helium ions on Al are proportional to the velocity. Our results indicate the linearity of the electronic stopping power of slow He ions in aluminum.

*Corresponding author: riccardi@fis.unical.it
†Deceased.

II. EXPERIMENTS

The experiments were performed in an ultrahigh vacuum ($\sim 10^{-10}$ mbar) system used in previous electron emission studies [15]. Electrons ejected from the Al sample were energy analyzed with a double-pass cylindrical mirror spectrometer operated inside a magnetic shield at a constant pass energy of 50 eV and a resolution of 0.2 eV. The surfaces of the samples were normal to the axis of the spectrometer and at 12° with respect to the ion beam direction. In this geometry, the spectrometer collects electrons emitted in a cone around 43° to the surface normal. Helium ions were produced in an electron impact source, operated with 58 eV electrons. Similar results were obtained using 30 eV electrons in the ion source, indicating negligible contamination of the ion beam with doubly charged ions. The high-purity polycrystalline Al surfaces were sputter cleaned by 4 keV Ar^+ ions at 12° glancing incidence. The sputtering was continued beyond that required to remove any detectable level of contamination by Auger spectroscopy and until the structure in the electron energy spectra became constant.

III. ELECTRON ENERGY DISTRIBUTIONS

In Fig. 1 we report the energy distributions of electrons emitted from Al surfaces by $^3He^+$ ions as a function of incident energy. Ions were impinged on the surface at an incidence angle $\Theta_i = 78°$ and the observation angle was $\Theta_i = 0°$ (the angles are measured with respect to the surface normal). The spectra have been normalized to the beam current measured on the sample under positive bias and are consistent with the spectra of electron emission that was previously reported in the literature [15–17]. At low impact energy the spectra are

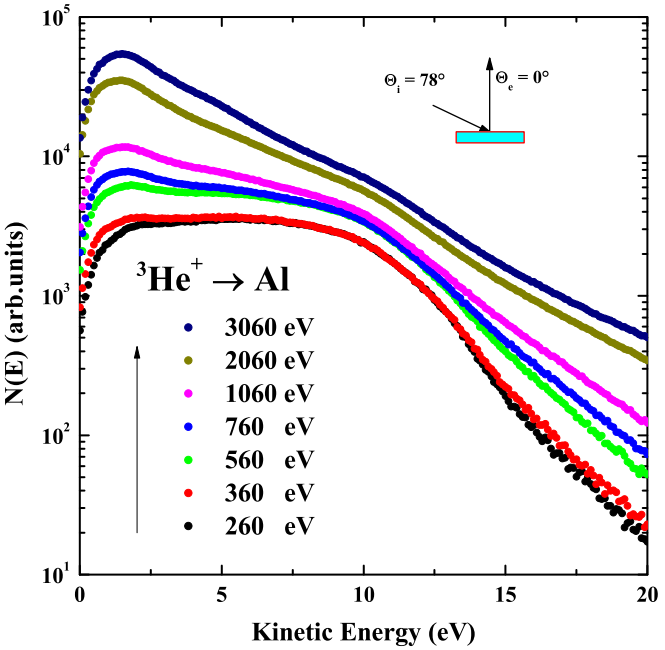

FIG. 1. (Color online) Energy spectra $N(E)$ of electrons emitted from the Al surface by $^3He^+$ impact. The spectra have been normalized to the beam current measured on the sample under positive bias. The inset shows a simple schematic of the experimental geometry.

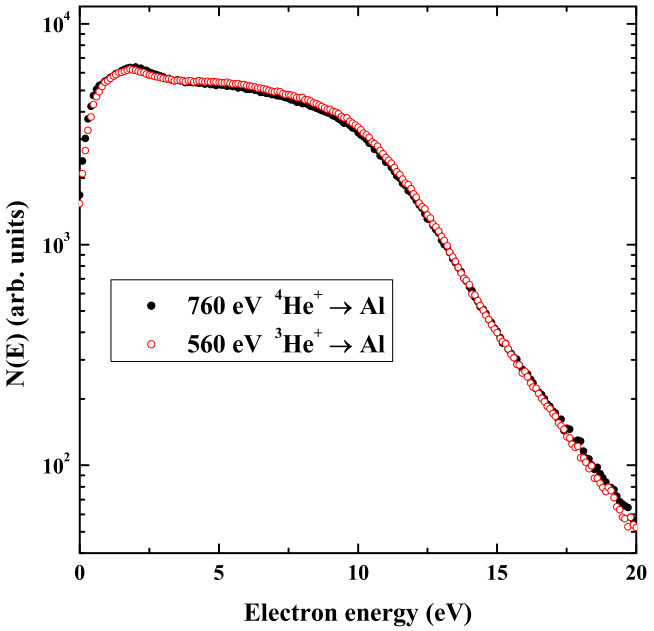

FIG. 2. (Color online) Comparison of energy spectra of electrons excited by $^3He^+$ and $^4He^+$ at similar velocities. The spectra have been normalized to the beam current measured on the sample under positive bias.

dominated by PEE [15,16]. In this mechanism, excitation results when the potential energy stored in the projectile ion is released when the incoming ion is neutralized by Auger capture and plasmon-assisted neutralization [10,15]. With increasing impact energy, the spectra in Fig. 1 show the transition from the potential to the kinetic emission regime. The spectra of kinetic electron emission are characterized by a low-energy peak, followed by a monotonically decreasing tail due to electrons excited in the collisional electronic cascade inside the solid [11]. The cascade feature constitutes the background on which two distinct features, attributed to low momentum surface and bulk plasmons, are superimposed [17].

Velocity dependent effects in the potential and the kinetic regime are illustrated in Figs. 2 and 3, respectively. Figure 2 reports the comparison between the energy distribution $N(E)$ for the 560 eV $^3He^+$ and 760 eV $^4He^+$ impact on Al. The spectra in Fig. 2 are dominated by PEE, and velocity dependent effects are observed in the high-energy tail of the electron spectrum due to the Auger neutralization of the incoming ions [10,15,16]. In the Auger neutralization process, electrons are emitted in a spectrum with a maximum energy E_b given by $E_b = I' - 2\Phi$ [16] (where I' is the ionization potential of the parent atom shifted by the image interaction and Φ is the metal work function), corresponding to the case where the two electrons participating in the Auger process are at the Fermi level. This high-energy edge is broadened by the atomic energy level shift near the surface and incomplete adiabaticity caused by the ion velocity normal to the surface [16,18]. Therefore, in the PEE regime, $^3He^+$ ions and $^4He^+$ ions of similar velocity produce a similar broadening, as shown by the high-energy tailing of the spectra in Fig. 2.

Figure 3 compares the electron emission spectra induced by 3 keV $^3He^+$ with that excited by the impact of 4 keV $^3He^+$ and $^3He^+$ on Al and by 1 keV electrons. At these impact energies,

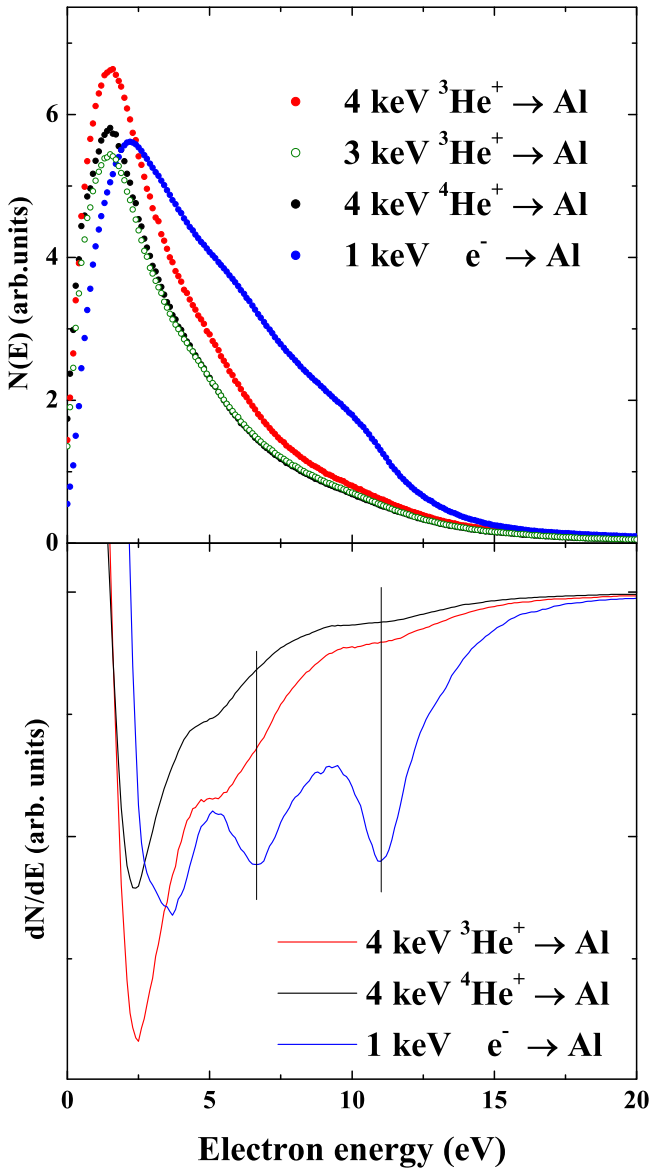

FIG. 3. (Color online) Top: Energy spectra of electrons emitted by the Al surface bombarded by 3 keV ^{3}He$^+$, 4 keV ^{3}He$^+$, and ^{4}He$^+$, and by 1 keV electrons. The ion-induced spectra are normalized to the beam current. The electron-induced spectrum has been arbitrarily rescaled to compare line shapes. Bottom: Derivative $dN(E)/dE$. The vertical bars indicate the position of the surface and bulk plasmon features.

ion-induced spectra reveal evidence of bulk and surface plasmon excitation and decay [17], as shown by the comparison with the spectrum induced by 1 keV electrons, commonly used as a benchmark to individuate these excitations [17]. The plasmon structures are better visualized in the derivative of the spectrum [15], dN/dE, where they result in the minima at energies $E_m = E_{\rm pl} - \Phi$, 6.5 and 11 eV, corresponding respectively to the surface and bulk plasmon ($\Phi = 4.3$ eV is the work function for polycrystalline Al). These observations are consistent with previous studies of subthreshold plasmon excitation by fast secondary electrons excited by the kinetic energy transfer of incoming particles [17].

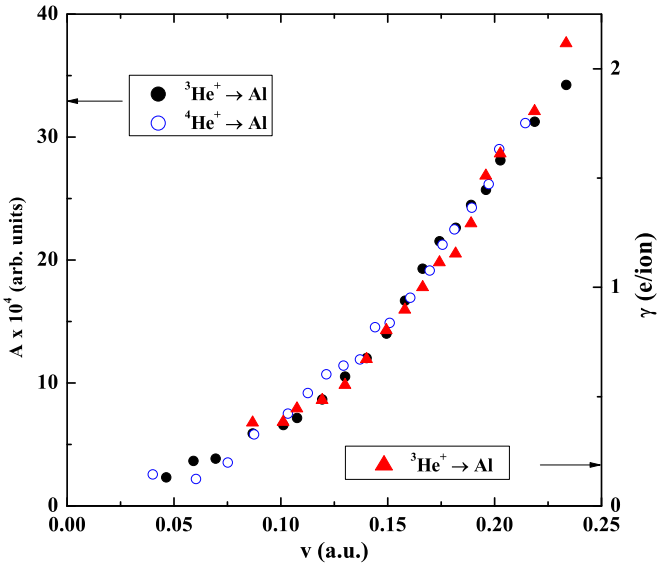

FIG. 4. (Color online) Electron emission yields γ for $\Theta_i = 78^\circ$ vs v, the velocity of the projectile. A is the area of the spectra in Fig. 1. The yield was evaluated, with about a 15% uncertainty, by measuring the current on the sample under positive and negative bias.

IV. ELECTRON EMISSION INTENSITY

Figure 3 shows that the area of the spectrum excited by 4 KeV ^{4}He$^+$ is ∼18% smaller than that of the spectrum excited by ^{3}He at the same energy but closer (3% larger) to that of the spectrum excited by ^{3}He at 3 keV, i.e., at the same velocity. This appears consistent with the 15% larger velocity of ^{3}He due to the mass ratio of the two isotopes ($\sqrt{4/3}$), and indicates a dependence of KEE intensity on velocity, rather than on energy, in agreement with the absence of isotope effects in electron emission by protons and deuterons [12]. To further discuss this issue, we report in Fig. 4 the electron emission yields as a function of projectile velocity, measured during our experiments for ^{3}He and ^{4}He ion impacts.

Electron emission yields have been measured during bombardment by recording the currents on the sample under positive and negative bias. Also reported for comparison are the areas of the measured energy spectra, to show that they give the same information. The yields enter the kinetic regime at an apparent impact velocity of about 0.1 a.u. and approach a linear behavior with increasing ion velocity, though the threshold behavior is quite smooth and there is an extended range of velocity where both PEE and KEE coexist, as is already evident in Fig. 1. The important point here is that kinetic emission yields show the same threshold and the same dependence on velocity for both projectiles in the entire range investigated. This would not be the case if charge exchange processes due to electron promotion of the He 1s level were important in determining electron emission. Projectile ionization due to electron promotion requires a threshold distance of the closest approach to be reached during a binary collision. This distance depends on the impact energy and, being the same for both projectiles, would be reached at a lower velocity by the heavier projectile. In contrast, the observations reported in Figs. 1–4 indicate a clear dependence of the emission yields on projectile velocity, rather than on energy.

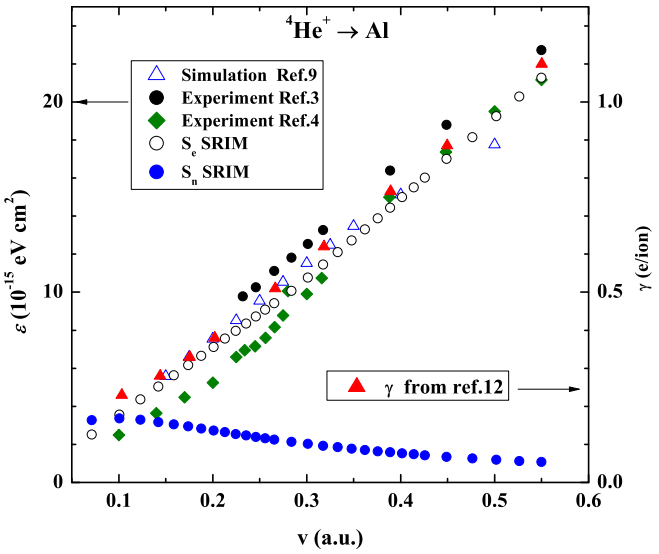

FIG. 5. (Color online) Comparison of the electron emission yields γ for $\Theta_i = 0^\circ$ [12] with electronic stopping cross sections ($\varepsilon = S_e/n$, where n is the atomic number density) from Refs. [3,4,9]. Note the proportionality by a factor 20 between the two vertical scales. Also shown are the nuclear and electronic stopping powers given by SRIM.

The results reported in Fig. 4 compare well with previous measurements of electron emission yields under the impact of ^{4}He ions on Al at normal incidence [12], reported in Fig. 5. The yields show the proportionality to velocity up to an energy of 30 keV. The yields measured at normal incidence are lower than those reported in this work because of the small electron escape depth. At glancing angles, the projectiles deposit more energy at shallower depths than near normal incidence. The results reported in Figs. 4 and 5 are consistent with the angular dependence observed for He ion impact on metal surfaces [19], which showed a dependence of the type $[\cos(\Theta_i)]^{-f}$, with the exponent f close to but generally different from unity and strongly dependent on the projectile target combination and on impact energy.

Thus, there are two facts that exclude a significant contribution to the electron emission induced by the impact of He ions on Al of electron promotion above the vacuum level in close atomic collisions. The first is that the dependence on velocity of the emission yields is the same for both He isotopes. The second is that deviations from linearity of the emission yields, which could signal the onset of additional processes, have not been observed over an extended range of impact energies, from 2 to 40 keV, as shown in Fig. 5. It is important to remark that our findings do not imply that promotion effects are absent. Electron promotion and charge exchange processes have been indeed observed either in He-Al asymmetric collisions or in symmetric collisions between recoiling target atoms [20]. However, these processes become important at impact energies below the threshold for direct excitation of valence electrons, i.e., for projectiles heavier than helium [13,14]. We conclude that kinetic electron emission under the impact of helium ions on Al is dominated by the escape of excited electrons produced by direct binary collisions between the projectile and the valence electrons of the target.

V. COMPARISON WITH ELECTRONIC STOPPING POWER DATA

The conclusion of the foregoing discussion has important implications on the debate about electronic stopping power. Figure 5 shows also the electronic stopping power for He in Al reported by Primetzhofer *et al.* [4]. This curve has been obtained combining two sets of data: those acquired at low velocity in the backscattering experiments [4] and the linear behavior at high velocity taken from an earlier work by Ormrod *et al.* [21], who performed transmission experiments in the impact energy range 15–65 keV. The electronic stopping power in Ref. [4] has been also compared and reported to be consistent with DFT calculations [22,23] that slightly overestimate the measured electronic stopping power at low energy by 13%. Here, we further compare this electronic stopping curve with that reported in the transmission experiments by Martinez-Tamayo *et al.* [3] and with the electronic stopping power for He ions in Al calculated by TDDFT [9]. We point out that the linear dependence at high velocity in Ref. [4] is the same as the data of the transmission experiments by Martinez-Tamayo *et al.* [3]. These last data, however, do not show any deviation from linearity at low velocity, in a range overlapping with that of the measurements in backscattering of Ref. [4]. We include in Fig. 5 also the electronic stopping power from tables used by the SRIM code (stopping and range of ions in matter) [24] that shows the same linear behavior as the data by Martinez-Tamayo *et al.* [3] and Ormrod *et al.* [21]. More interestingly, the linear dependence of these experimental data turned out to be in excellent agreement at low velocity also with the electronic stopping power for He ions in Al calculated by TDDFT [9]. This observation is remarkable because DFT calculations were not expected to adequately describe the slope at high velocity of the electronic stopping power [4] as they consider only the valence electron excitation. The agreement between experimental data and TDDFT calculation was not previously realized [9] and might be significant in view of the important effort recently performed to improve the description of the energy loss of slow ions in solids by DFT calculations [7–9]. In this sense, we mention that the slope of the stopping power calculated by TDDFT shows a slight decrease at the highest velocity that it is observed also in the stopping measurements [3] but at higher energies.

As mentioned above, the experimental curves of the electronic stopping power are in good agreement only at high impact velocity, above about 0.3 a.u., and show the same linear dependence on velocity. In both cases the ratios γ/S_e are constant with very low uncertainties well within 3%; the slight 10% offset between the two curves has no significant effect on their proportionality to the experimental electron emission yields in Ref. [12]. The proportionality between emission yields and the high-energy range of the stopping power reported in Ref. [4] is evidentiated in Fig. 5, where a proportionality factor of 20 has been adopted for the two vertical scales. On the other side, the electronic stopping power measured in backscattering [4] is not linear at low energy and the ratio γ/S_e decreases by more than 30% with increasing energy in the range 2–10 keV. The interpretation of the results by Primetzhofer *et al.* [4] implies that electrons

are promoted only at energies below the vacuum level so that electron emission experiments do not reveal the process. In contrast, the linearity of the electronic stopping power reported by Martinez-Tamayo *et al.* [3] is fully consistent with the results of electron emission experiments and does not require additional mechanisms to be explained. This, in turn, implies that electron emission is a proper probe for the electronic stopping of He ions in Al, though detecting only a fraction of the excited electrons.

A discussion of the discrepancy at low energy between measurements of the electronic stopping power has not been given. It has been stated [6] that results of the transmission experiments could be reproduced by adding a nuclear stopping correction to the results of the experiments in backscattering. For comparison, in Fig. 5 we report also the nuclear stopping power from tables used by the SRIM code [24]. The nuclear stopping power calculated by SRIM shows a maximum at $v \sim 0.1$ a.u. In contrast, and judging from the differences between the curves in Fig. 5, the claimed nuclear stopping correction would require a maximum of similar magnitude but shifted to a higher velocity of $\sim$0.2 a.u. Thus, it is likely that the discrepancy in the measured electronic stopping power originates in the difficulty in disentangling the role of the nuclear contribution in the backscattering experiments.

VI. CONCLUSIONS

We have reported energy distribution and yields of electron emission in the interaction of $^3He^+$ and $^4He^+$ ions with an Al surface. The intensity of emission shows the same dependence on velocity for the two isotopes. This implies that electron promotion effects do not produce a significant contribution and the KEE yields for the impact of helium ions on Al are dominated by direct excitation of the valence electrons. A comparison with reported electronic stopping power indicates the linearity of the electronic stopping with the projectile velocity, showing that electron emission yields can provide an indirect measure of the energy transferred by incoming particles to the electronic subsystem that is not affected by the contribution of the nuclear stopping. The comparison shows the consistency of a whole set of results to a simple physical picture for the electronic stopping of He ions in Al that do not require an important contribution of electron promotion effects that, therefore, appear unconvincingly established also in consideration of decades of the relevant literature.

[1] P. Sigmund, *Particle Penetration and Radiation Effects*, Springer Series in Solid-State Sciences Vol. 151 (Springer, Berlin, 2006).

[2] P. Sigmund, *Particle Penetration and Radiation Effects, Volume 2*, Springer Series in Solid-State Sciences Vol. 179 (Springer, Berlin, 2014).

[3] G. Martinez-Tamayo, J. C. Eckardt, G. H. Lantschner, and N. R. Arista, Phys. Rev. A **54**, 3131 (1996).

[4] D. Primetzhofer, S. Rund, D. Roth, D. Goebl, and P. Bauer, Phys. Rev. Lett. **107**, 163201 (2011).

[5] D. Goebl, K. Khalal-Kouache, D. Roth, E. Steinbauer, and P. Bauer, Phys. Rev. A **88**, 032901 (2013).

[6] H. Paul, in *Application of Accelerators in Research and Industry: Twenty-Second International Conference*, edited by F. D. McDaniel, B. L. Doyle, G. A. Glass, and Y. Wang, AIP Conf. Proc. No. 1525 (AIP, Melville, NY, 2013), p. 309.

[7] A. A. Correa, J. Kohanoff, E. Artacho, D. Sanchez-Portal, and A. Caro, Phys. Rev. Lett. **108**, 213201 (2012).

[8] M. A. Zeb, J. Kohanoff, D. Sanchez-Portal, A. Arnau, J. I. Juaristi, and E. Artacho, Phys. Rev. Lett. **108**, 225504 (2012).

[9] M. Ahnsan Zeb, J. Kohanoff, D. Sanchez-Portal, and E. Artacho, Nucl. Instrum Methods B **303**, 59 (2013).

[10] R. C. Monreal, Prog. Surf. Sci. **89**, 80 (2014).

[11] R. A. Baragiola and P. Riccardi, in *Reactive Sputter Deposition*, edited by D. Depla and S. Mahieu, Springer Series in Materials Science Vol. 109 (Springer, Berlin, 2008), Chap. 2.

[12] R. A. Baragiola, E. V. Alonso, and A. Oliva Florio, Phys. Rev. B **19**, 121 (1979).

[13] J. W. Rabalais, H. Bu, and C. D. Roux, Phys. Rev. Lett. **69**, 1391 (1992).

[14] M. Minniti, M. Commisso, A. Sindona, E. Sicilia, A. Bonanno, P. Barone, R. A. Baragiola, and P. Riccardi, Phys. Rev. B **75**, 045424 (2007).

[15] R. A. Baragiola and C. A. Dukes, Phys. Rev. Lett. **76**, 2547 (1996).

[16] P. Barone, A. Sindona, R. A. Baragiola, A. Bonanno, A. Oliva, and P. Riccardi, Nucl. Instrum Methods B **209**, 68 (2003).

[17] R. A. Baragiola, C. A. Dukes, and P. Riccardi, Nucl. Instrum Methods B **182**, 73 (2001).

[18] A. Sindona, R. A. Baragiola, G. Falcone, A. Oliva, and P. Riccardi, Phys. Rev. A **71**, 052903 (2005).

[19] J. Ferron, E. V. Alonso, R. A. Baragiola, and A. Oliva-Florio, Phys. Rev. B **24**, 4412 (1981).

[20] R. A. Baragiola, E. V. Alonso, and H. J. L. Raiti, Phys. Rev. A **25**, 1969 (1982).

[21] J. H. Ormrod, J. R. Mac Donald, and H. E. Duckworth, Can. J. Phys. **43**, 275 (1965).

[22] N. P. Wang and I. Nagy, Phys. Rev. A **56**, 4795 (1997).

[23] E. A. Figueroa and N. R. Arista, J. Phys.: Condens. Matter **22**, 015602 (2010).

[24] J. F. Ziegler, SRIM 2003–SRIM 2013, available from http://www.srim.org